



Reduction of Multiple Scattering to Second Order Scattering for Determination of Liquid-Cloud Microphysical Properties

Xiaoying Cao¹, Gilles Roy² and Grégoire Tremblay³

¹ Lidar Consultant, Ottawa

² Defence Research and Development Canada - Valcartier Research Centre

³ AEREX Avionic, Levis

28th International Laser Radar Conference
25–30 June 2017 Politehnica University of Bucharest

Defence Research and Development Canada

External Literature (N)

DRDC-RDDC-2018-N006

February 2018

CAN UNCLASSIFIED

IMPORTANT INFORMATIVE STATEMENTS

Disclaimer: This document is not published by the Editorial Office of Defence Research and Development Canada, an agency of the Department of National Defence of Canada, but is to be catalogued in the Canadian Defence Information System (CANDIS), the national repository for Defence S&T documents. Her Majesty the Queen in Right of Canada (Department of National Defence) makes no representations or warranties, expressed or implied, of any kind whatsoever, and assumes no liability for the accuracy, reliability, completeness, currency or usefulness of any information, product, process or material included in this document. Nothing in this document should be interpreted as an endorsement for the specific use of any tool, technique or process examined in it. Any reliance on, or use of, any information, product, process or material included in this document is at the sole risk of the person so using it or relying on it. Canada does not assume any liability in respect of any damages or losses arising out of or in connection with the use of, or reliance on, any information, product, process or material included in this document.

This document was reviewed for Controlled Goods by Defence Research and Development Canada (DRDC) using the Schedule to the *Defence Production Act*.

© Her Majesty the Queen in Right of Canada (Department of National Defence), 2017

© Sa Majesté la Reine en droit du Canada (Ministère de la Défense nationale), 2017

CAN UNCLASSIFIED

REDUCTION OF MULTIPLE SCATTERING TO SECOND ORDER SCATTERING FOR DETERMINATION OF LIQUID-CLOUD MICROPHYSICAL PROPERTIES

Xiaoying Cao¹, Gilles Roy^{2*} and Grégoire Tremblay³

¹Lidar Consultant, Ottawa, Canada; ^{2*}RDDC Valcartier 2459 de la Bravoure, Québec, Qc, Canada, gilles.roy@drdc-rddc.gc.ca

³AEREX Avionic, Levis, Canada;

ABSTRACT

Under single scattering conditions, water droplets clouds do not depolarize the backscattered light. However, backscattered light from multiple scattering will be depolarized. The level of depolarization is a function of the droplets size and of the cloud extinction coefficient value and its profile; it has also a strong dependency on the lidar field-of-view (FOV) and azimuth angle [1]-[3]. It has been demonstrated in [4] that the multiple scattering cross polarization signal can be reduced to a second order scattering one using the azimuthal dependency of the cross polarization. In this paper we present how the multiple scattering cross polarization can be reduced to a second order scattering and how this signal is related to the droplet particle size. Monte Carlo simulations for clouds at different ranges and effective radius sizes are performed and compared with the results obtained with an analytical model.

1. AZIMUTHAL CROSS POLARIZATION PATTERN

Backscattered light from spherical particles does not change the polarization orientation state of a linearly polarized incident light. This particularity allows the discrimination of spherical particles from non-spherical particles. However, under multiple scattering conditions, even spherical particles do generate depolarized signals. In fact, the multiple scattering cross polarization shows an azimuthal pattern. This pattern is easily observed using a gated ICCD camera and a polarized beam splitter as shown in Fig. 1. A linearly polarized parallel laser beam is used. At the reception, after collimation, the cross polarization is imaged on the detector. An adjustable delay is used to image the backscattered light from the cloud from a specific cloud depth. The gate width of the ICCD is typically 10 to 20 ns. Please refer to [1] for relevant details.

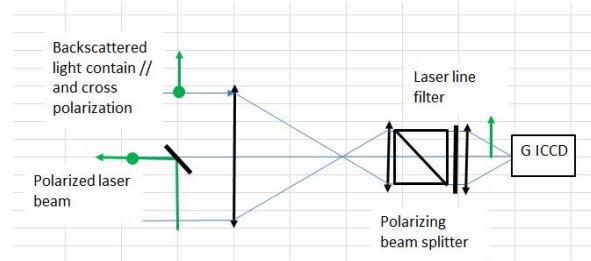


Figure 1. Lidar set up to capture the azimuthal cross polarization. The linearly polarized source is emitted on axis (lower left). The received signal is collimated through a polarizer and the cross polarization is imaged on the camera (right).

In order to better understand the mechanism of polarized multiple scattering, Monte Carlo (MC) simulation has been performed. The Undique MC simulator is a multithreaded software based on the Bohren and Huffman Mie scattering algorithm. The simulator reproduces the characteristics of a Flash Lidar system. It consists of an emitter/receiver system, a target and a propagation range including aerosols of various properties. The particularity of the Undique MC is its capability to image the scattered light on a detector array [5]. Fig. 2 shows the azimuthal pattern obtained for the simulation of a penetration of 50 m in a cloud of constant extinction 0.03 m^{-1} starting at 1000 m. The image at the top contains all the scattering orders, while the image at the bottom contains second order scattering only. The second order scattering cross polarization follows a $\text{Cos}(4\varphi)$ pattern; it means there is no second-order scattered energy for azimuths equal to 0° , 90° , 180° , 270° . In multiple scattering conditions (top part of Fig. 2) there clearly is a fair amount of energy at those angles. The subtraction of the higher order scattering energy found at those specific angles, when done at all azimuths, leads to a second order scattering pattern [4]. So, it appears that multiple scattering effects occurring in dense water cloud can be simplified to second

order scattering. In the following, we will examine what are the mechanisms leading to depolarization of the lidar signal from second order scattering.

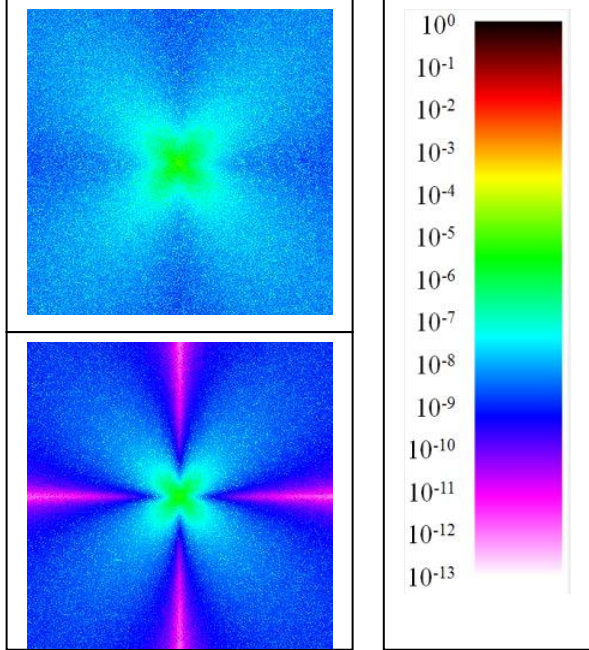


Figure 2. Monte Carlo simulation of cross polarization azimuthal pattern. The top image contains all orders scattering. The image at the bottom is for second order scattering only.

2. BACKSCATTERING AND DEPOLARIZATION

Lidars with polarization capabilities usually work at a specific FOV and detect the parallel and cross polarization components of the lidar return. The lidar signals will contain all scattering orders. In this paper, we want to reduce multiple scattering effects to second order scattering. To do so, it is necessary to have a look at the Mie scattering phase function and how the scattered light is depolarized.

The linear depolarization ratio (δ_{lin}) at a scattering angle β is defined as the ratio of the power integrated over the azimuthal angles φ in the plane of polarization orthogonal (I_{\perp}) and parallel (I_{\parallel}) to the linearly polarized source:

$$\delta_{lin}(\beta) = \frac{\langle I_{\perp} \rangle}{\langle I_{\parallel} \rangle} = \frac{\int_0^{2\pi} I_y(\beta, \varphi) d\varphi}{\int_0^{2\pi} I_x(\beta, \varphi) d\varphi}. \quad (1)$$

Using Mie theory, it can be shown that:

$$\delta_{lin}(\beta) = \frac{(P_2 \cos^2 \beta - 2P_3 \cos \beta + P_1)}{(3P_2 \cos^2 \beta + 2P_3 \cos \beta + 3P_1)}, \quad (2)$$

where in P_1 , P_2 and P_3 are the Mie scattering phase matrix elements defined by Deirmendjian.

Fig. 3 shows the phase function and the depolarization ratio at a wavelength of $0.532 \mu\text{m}$ for linear incident waves on water-droplets of effective radius of $6 \mu\text{m}$. The water droplets size distribution is a gamma distribution with $\alpha = 7$ and $\beta = 1.5$.

For depolarization, the major observations are:

- 1) The light is not depolarized in the forward scattering direction for angles smaller than 20° ;
- 2) the depolarization is equal to 0 at 180° ;
- 3) the depolarization increases very sharply around 180° .

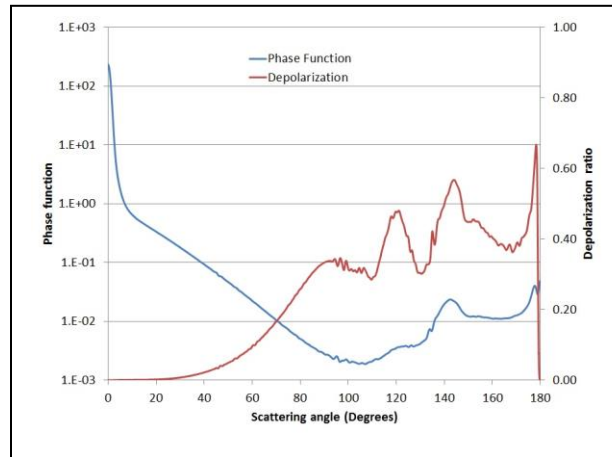


Figure 3. Phase functions and linear depolarization ratio for a water droplets gamma distribution with effective radius of $6 \mu\text{m}$.

So, for a lidar, depolarization is mainly caused by a backscattering occurring after one or many forward scatterings as illustrated in Fig. 4.

A lidar with a given FOV (θ_i) will measure the backscattered light without any distinction regarding the forward scattering event position in space. The cross polarized second order scattering signal detected will be the sum of all those signals and it will be given by:

$$P_{D_{\perp}}(z_c, \theta_i) = P(z_c) \int_0^{z_c} \int_0^{\beta_i} F(z, \beta) \sin \beta d\beta dz$$

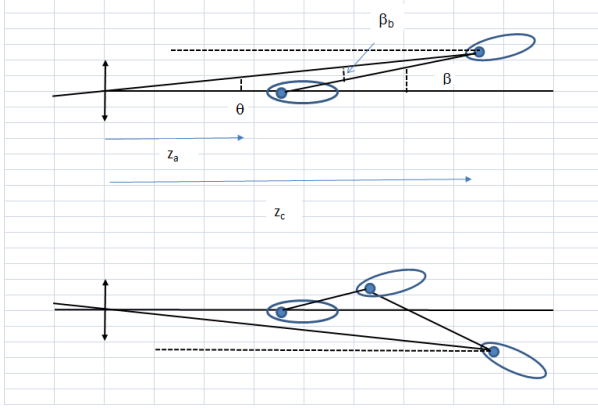


Figure 4. Double scattering processes and higher scattering processes leading to backscattering depolarization.

where $P(z_c) = P_0 \exp\left[-2 \int_0^{z_c} \alpha(z) dz\right] \frac{c \tau}{2} \frac{4\pi A}{z_c^2}$, and

$$F(z, \beta) = [\alpha_s(z) p(r, \beta)] [\alpha_s(z_c) p_{\perp}(r, \beta_b)],$$

where, c , τ and A are respectively the speed of light, the pulse width, and the collecting optics area; α_s is the scattering extinction coefficient; $p(r, z, \beta)$ is the value of the phase function for the forward scattering (β), and $p_{\perp}(r, z_c, \beta_b)$ the value of the perpendicular components of the phase function at backward scattering angles ($\beta_b = \pi - \beta + \theta$) for a particle of radius r ; z_a is where the cloud starts; z_c is the distance where the scattered radiation is measured; the quantity $[\alpha_s(z) p(r, z, \beta)]$ represents the forward scattering coefficient while $[\alpha_s(z_c) p_{\perp}(r, z_c, \beta_b)]$ represents the cross polarization backscattering coefficient. The FOV θ is easily related to the scattering angle β via: $\tan \beta = (z_c \tan \theta) / (z_c - z)$.

The forward scattering phase function is modelled as a summation of Gaussians [6]

$$p(r, \beta) = \frac{1}{2} \frac{1}{\pi \beta_d} \exp(-\beta^2 / \beta_d^2) + \frac{A_g}{2} \frac{1}{\pi \beta_g} \exp(-\beta^2 / \beta_g^2)$$

$$\beta_d = 0.585 (\lambda / 2r_e); \beta_g = 0.481; A_g = 0.89;$$

r_e : effective radius, λ : wavelength.

There is no existing model for $p_{\perp}(r, \beta_b)$, the perpendicular components of the phase function.

Our analysis has lead us rather to use the depolarization parameter ($D = p_{\perp} / (p_{\perp} + p_{\parallel})$) rather than $p_{\perp}(r, \beta_b)$. Fig. 5 shows the definition of various parameters used to express the depolarization parameter as a function of scattering angles ranging from 170° to 180° . The complete derivation of the parameterization for r_e ranging from 2 to $12\mu\text{m}$ will be published in *Appl. Opt* in 2017. The mathematical representation is as follows:

$$\beta_{Max}(r_e) = 1.5845 \ln(r_e) + 175.09^{\circ}$$

If, $\beta \geq \beta_{Max}(r_e)$

$$D(\beta, r_e) = A(r_e) [1 - \exp(-((\pi - \beta) / (\beta_d(r_e) w(r_e)))^4)]$$

$$w(r_e) = 0.4625 + 0.10485 r_e$$

If, $\beta < \beta_{Max}(r_e)$

$$D(\beta, r_e) = B_1(r_e) \cdot \exp(-B_3(0.944 \pi - (\pi - \beta)) + B_2(r_e))$$

In short, $D(\beta, r_e)$ starts from a value of zero at 180° and increases quickly following a super-Gaussian. It needs to be noted here that the width of the super-Gaussian is directly related to the width of the forward scattering peak β_d . Past the maximum value, in the direction of decreasing angles, $D(\beta, r_e)$ decreases exponentially.

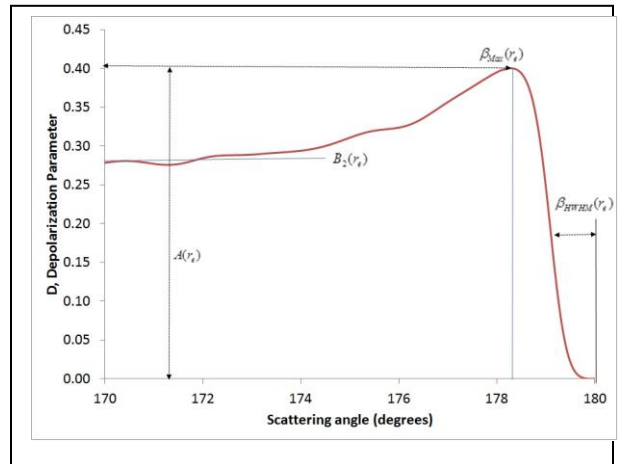


Figure 5. Parameterization of backscattering depolarization parameter. A water droplet cloud of effective radius of $6\mu\text{m}$ is represented.

3. RESULTS

Fig. 6 shows the calculated and normalized detected energy in rings delimited by FOV θ_i

around the backscatter direction and for effective particle radius of $6\ \mu\text{m}$. It is obtained using the model previously described (see Fig. 5) for a wavelength of $532\ \text{nm}$, beam divergence: $0.3\ \text{mrad}$, pulse width: $5\ \text{ns}$, cloud base: $100\ \text{m}$, depth: $20\ \text{m}$, extinction coefficient equal to $0.25\ \text{m}^{-1}$.

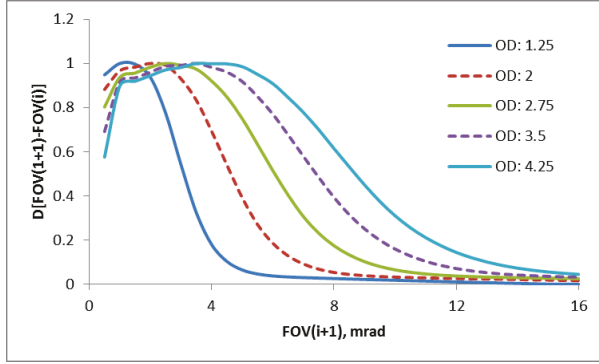


Figure 6. From 2nd scattering polarimetric model. Detected energy in rings delimited by FOV θ_i and θ_{i+1} for effective particle radius $6\ \mu\text{m}$.

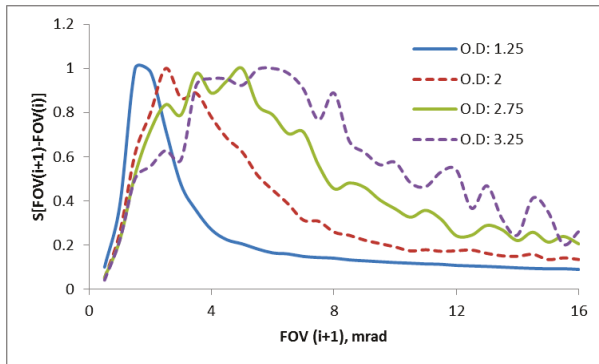


Figure 7. From MC simulation. Detected energy in rings delimited by FOV θ_i and θ_{i+1} for effective particle radius $6\ \mu\text{m}$

Using the same cloud parameters and lidar characteristics as for the model calculation displayed in Fig. 6, MC simulations were performed and images were analysed to recover second order scattering. Figure 7 shows the calculated and normalized detected energy in rings delimited by FOV θ_i and θ_{i+1} . Fig. 8 shows a clear dependency of the polarimetric signal over the droplet size

The MC results are noisier for the larger optical depths. The MC results and polarimetry double scattering model agree reasonably well in shape.

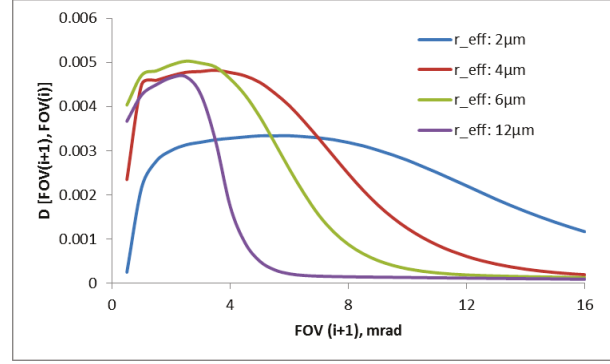


Figure 8. From 2nd scattering polarimetric model. Detected energy in ring delimited by FOV θ_i and θ_{i+1} for effective particle radius $2, 4, 6$ & $12\ \mu\text{m}$. Same cloud extinction and position as Fig. 6 and Fig. 7. Penetration depth is of $11\ \text{m}$.

CONCLUSION

Monte Carlo simulations support experimental observations reported in [1]; i.e. multiple scattering cross polarization can be reduced to a second order scattering using the azimuthal dependency of the secondary polarization. A model of the polarimetric backscattering phase function has led to a mathematical expression for the polarimetric backscatter signal. This signal can be related to the droplet particle size. Future work will focus on the extraction of the droplet size.

REFERENCES

- [1] S. R. Pal and A. I., Carswell, Polarization anisotropy in lidar multiple scattering from atmospheric clouds, *Appl. Opt.*, **24**, 3464-3471 (1985).
- [2] V. Griaznov, I. Veselovskii, P. Girolamo, M. Korenskii and D. Summa, Spatial distribution of doubly scattered polarized laser radiation in the focal plane of a lidar receiver, *Appl. Opt.* **46**, 6821-6830, (2007)
- [3] N. Roy, G. Roy, L. R. Bissonnette and J-R. Simard, Measurement of the azimuthal dependence of cross-polarized lidar returns and its relation to optical depth, *Appl. Opt.* **43**, 2777-2785, (2004)
- [4] A. Doroshkevich, The effect of droplet cloudy microstructure on the polarization characteristics of double scattering lidar return, *SPIE* Vol. 10035, 1003550, (2016)
- [5] G. Tremblay, G. Roy, High fidelity imaging algorithm for the Undique Monte Carlo simulator. *27rd International Laser Radar Conference*, New York, USA, (2015)
- [6] Luc R. Bissonnette, Gilles Roy, Laurent Poutier, Stewart G. Cober, and George A. Isaac, Multiple-scattering lidar retrieval method: tests on Monte Carlo simulations and comparisons with in situ measurements, *Appl. Opt.*, **41**, (2002)

DOCUMENT CONTROL DATA		
(Security markings for the title, abstract and indexing annotation must be entered when the document is Classified or Designated)		
<p>1. ORIGINATOR (The name and address of the organization preparing the document. Organizations for whom the document was prepared, e.g., Centre sponsoring a contractor's report, or tasking agency, are entered in Section 8.)</p> <p>DRDC – Valcartier Research Centre Defence Research and Development Canada 2459 route de la Bravoure Quebec (Quebec) G3J 1X5 Canada</p>	<p>2a. SECURITY MARKING (Overall security marking of the document including special supplemental markings if applicable.)</p> <p style="text-align: center;">CAN UNCLASSIFIED</p>	
	<p>2b. CONTROLLED GOODS</p> <p style="text-align: center;">NON-CONTROLLED GOODS DMC A</p>	
<p>3. TITLE (The complete document title as indicated on the title page. Its classification should be indicated by the appropriate abbreviation (S, C or U) in parentheses after the title.)</p> <p style="text-align: center;">Reduction of Multiple Scattering to Second Order Scattering for Determination of Liquid-Cloud Microphysical Properties</p>		
<p>4. AUTHORS (last name, followed by initials – ranks, titles, etc., not to be used)</p> <p style="text-align: center;">Cao, X.; Roy, G.; Tremblay, G.</p>		
<p>5. DATE OF PUBLICATION (Month and year of publication of document.)</p> <p style="text-align: center;">June 2017</p>	<p>6a. NO. OF PAGES (Total containing information, including Annexes, Appendices, etc.)</p> <p style="text-align: center;">4</p>	<p>6b. NO. OF REFS (Total cited in document.)</p> <p style="text-align: center;">6</p>
<p>7. DESCRIPTIVE NOTES (The category of the document, e.g., technical report, technical note or memorandum. If appropriate, enter the type of report, e.g., interim, progress, summary, annual or final. Give the inclusive dates when a specific reporting period is covered.)</p> <p style="text-align: center;">External Literature (N)</p>		
<p>8. SPONSORING ACTIVITY (The name of the department project office or laboratory sponsoring the research and development – include address.)</p> <p>DRDC – Valcartier Research Centre Defence Research and Development Canada 2459 route de la Bravoure Quebec (Quebec) G3J 1X5 Canada</p>		
<p>9a. PROJECT OR GRANT NO. (If appropriate, the applicable research and development project or grant number under which the document was written. Please specify whether project or grant.)</p> <p style="text-align: center;">03bb- Air Integrated - EO/IR SEN</p>	<p>9b. CONTRACT NO. (If appropriate, the applicable number under which the document was written.)</p>	
<p>10a. ORIGINATOR'S DOCUMENT NUMBER (The official document number by which the document is identified by the originating activity. This number must be unique to this document.)</p> <p style="text-align: center;">DRDC-RDDC-2018-N006</p>	<p>10b. OTHER DOCUMENT NO(s). (Any other numbers which may be assigned this document either by the originator or by the sponsor.)</p>	
<p>11a. FUTURE DISTRIBUTION (Any limitations on further dissemination of the document, other than those imposed by security classification.)</p> <p style="text-align: center;">Public release</p>		
<p>11b. FUTURE DISTRIBUTION OUTSIDE CANADA (Any limitations on further dissemination of the document, other than those imposed by security classification.)</p>		

12. **ABSTRACT** (A brief and factual summary of the document. It may also appear elsewhere in the body of the document itself. It is highly desirable that the abstract of classified documents be unclassified. Each paragraph of the abstract shall begin with an indication of the security classification of the information in the paragraph (unless the document itself is unclassified) represented as (S), (C), (R), or (U). It is not necessary to include here abstracts in both official languages unless the text is bilingual.)

Under single scattering conditions, water droplets clouds do not depolarize the backscattered light. However, backscattered light from multiple scattering will be depolarized. The level of depolarization is a function of the droplets size and of the cloud extinction coefficient value and its profile; it has also a strong dependency on the lidar field-of-view (FOV) and azimuth angle [1]- [3]. It has been demonstrated in [4] that the multiple scattering cross polarization signal can be reduced to a second order scattering one using the azimuthal dependency of the cross polarization. In this paper we present how the multiple scattering cross polarization can be reduced to a second order scattering and how this signal is related to the droplet particle size. Monte Carlo simulations for clouds at different ranges and effective radius sizes are performed and compared with the results obtained with an analytical model.

13. **KEYWORDS, DESCRIPTORS or IDENTIFIERS** (Technically meaningful terms or short phrases that characterize a document and could be helpful in cataloguing the document. They should be selected so that no security classification is required. Identifiers, such as equipment model designation, trade name, military project code name, geographic location may also be included. If possible keywords should be selected from a published thesaurus, e.g., Thesaurus of Engineering and Scientific Terms (TEST) and that thesaurus identified. If it is not possible to select indexing terms which are Unclassified, the classification of each should be indicated as with the title.)

Lidar, polarization, Multiple scattering